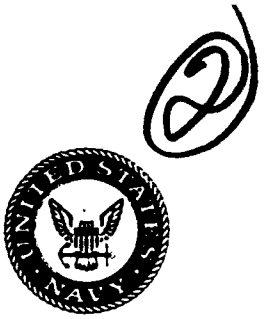

Naval Research Laboratory

Washington, DC 20375-5000

NRL/MR/4770—92-6974

Survey of Radioactivities Induced by Lithium Ions

FRANK C. YOUNG AND DAVID V. ROSE*

Pulsed Power Physics Branch
Plasma Physics Division

**JAYCOR*
Vienna, VA 22180-2270

June 15, 1992

REPORT DOCUMENTATION PAGE

Form Approved
OMB No. 0704-0188

1. AGENCY USE ONLY (Leave blank)	2. REPORT DATE	3. REPORT TYPE AND DATES COVERED
	June 15, 1992	Interim

4. TITLE AND SUBTITLE

Survey of Radioactivities Induced by Lithium Ions

5. FUNDING NUMBERS

SNL F.A.O. No. AA-9158

6. AUTHOR(S)

Frank C. Young and David V. Rose*

7. PERFORMING ORGANIZATION NAME(S) AND ADDRESS(ES)

Naval Research Laboratory
Washington, DC 20375-5000

8. PERFORMING ORGANIZATION REPORT NUMBER

NRL/MR/4770—92-6974

9. SPONSORING/MONITORING AGENCY NAME(S) AND ADDRESS(ES)

Sandia National Laboratories
Albuquerque, NM 87185

10. SPONSORING/MONITORING AGENCY REPORT NUMBER

11. SUPPLEMENTARY NOTES

*Jaycor, Vienna, VA 22180-2270

12a. DISTRIBUTION/AVAILABILITY STATEMENT

Approved for public release; distribution unlimited.

12b. DISTRIBUTION CODE

13. ABSTRACT *(Maximum 200 words)*

Lithium-induced nuclear reactions which lead to radioactivities are surveyed for application to experiments with intense lithium-ion beams from pulsed power generators. Positive Q-value reactions for ^{7}Li ions of up to 15 MeV on carbon, aluminum, steel, brass, and titanium alloy targets are identified. For each radioactivity, the half-life and decay products are tabulated. Reaction yields are dominated by the Coulomb barrier, and the scaling of the barrier penetration with ^{7}Li energy is evaluated for each target element.

14. SUBJECT TERMS

Lithium-induced nuclear reactions
Intense lithium beam
Radioactive products
Coulomb barrier penetrability

15. NUMBER OF PAGES
21

16. PRICE CODE

17. SECURITY CLASSIFICATION OF REPORT	18. SECURITY CLASSIFICATION OF THIS PAGE	19. SECURITY CLASSIFICATION OF ABSTRACT	20. LIMITATION OF ABSTRACT
UNCLASSIFIED	UNCLASSIFIED	UNCLASSIFIED	UL

Contents

SURVEY OF RADIOACTIVITIES INDUCED BY LITHIUM IONS

I. Introduction

Nuclear reactions produced by lithium ions which lead to radioactive products are surveyed for application to experiments with intense pulsed lithium beams. Experiments using lithium beams have been carried out at Sandia National Laboratories on the PBFA II generator and are planned for the Sabre generator. In this survey, radioactivities induced in the commonly used materials, carbon, aluminum, steel and brass, are identified. In addition, radioactivities induced in the alloy, titanium 6-4, are identified because this alloy is used in the ion-diode region of the Sabre generator. Experiments on the PBFA II generator indicate that the lithium beam is primarily singly-ionized ^{7}Li. This beam is produced from natural-abundance lithium which is primarily ^{7}Li (i.e., 92.5% ^{7}Li and 7.5% ^{6}Li). Therefore, reactions induced by ^{6}Li nuclei are not included in this survey. The diode voltage on the Sabre generator may be as high as 10 MV, and experiments on PBFA II have achieved voltages of up to 15 MV. Therefore, lithium beams with energies of up to 15 MeV are considered in this survey.

In Sec. II, the nuclear reactions on these targets which produce radioactivity are listed, and the decay properties of the radioactive nuclei are identified. In a survey of the published literature, measured yields have been reported only for one of these reactions, but measurements for other lithium-induced reactions indicate that the reaction yields are dominated by the Coulomb barrier in this energy range. Yield estimates based on Coulomb-barrier penetration are presented in Sec. III.

II. Survey of Nuclear Reactions

Nuclear reactions with positive Q-values which lead to radioactive residual nuclei are identified in this survey. Lithium-induced reactions leading to the following products are considered: n, p, d, t, ^{3}He, α, ^{6}Li and ^{6}He. The tabulation of Q-values by Keller et al.[1] is used as a guide to identify

Manuscript approved April 14, 1992.

positive Q-value reactions. Since the Q-values in Ref. 1 are listed with only two-significant-figure precision, the Q-values in this survey are calculated to four-significant-figure precision using atomic masses from Ref. 2. The reactions and their Q-values are listed in Table I for carbon and aluminum, in Table II for titanium 6-4 alloy, in Table III for steel, and in Table IV for brass. The natural abundance of each isotope is also listed.

For the alloy targets, this survey only includes target isotopes for which the product of the isotopic abundance and the alloy proportion exceeds 1%. The titanium 6-4 alloy consists of 90% titanium, 6% aluminum, and 4% vanadium. The steel target is assumed to be #304 stainless with a 70%-iron, 20%-chromium, and 10%-nickel composition. For brass, a 67%-copper and 33%-zinc composition is assumed. Each of these elements consists of several stable isotopes with significant fractional abundances. The target isotopes for which the product of the isotopic abundance and the alloy proportion exceeds 1% are expected to be the primary sources of radioactivity. In addition, reactions which produce the long-lived isotopes ^{53}Mn ($T_{\frac{1}{2}} = 3.7\times10^{6}$ yr), ^{59}Ni ($T_{\frac{1}{2}} = 8\times10^{4}$ yr), and ^{63}Ni ($T_{\frac{1}{2}} = 10^{2}$ yr) are not included in this survey. Unrealistically large ion-beam fluences would be required to produce significant activities of these long-lived isotopes. The decay mode of each residual nucleus is identified as β^- for electron decay, β^+ for positron decay, and ε for electron capture. For β-decay, E_β is the end-point energy of the β-spectrum, and E_γ is the energy of the most intense γ-ray(s) associated with the decay. The symbol ^{52m}Mn in Table II refers to a metastable state where ^{52}Mn is the ground state. The decay modes, half-lives, end-point energies and γ-ray energies are taken from Ref. 2. The most intense γ-decays are identified from Ref. 3.

III. Nuclear Reaction Yields

For each target isotope, at least one reaction with a positive Q-value of several MeV is listed. Reactions with positive Q-values are allowed by kinematics for any bombarding

Table I

Radioactivities Induced by ^{7}Li Ions on Carbon and Aluminum

Target		Nuclear Reaction		Residual Nucleus			
Isotope	Abundance	Reaction	Q-Value (MeV)	Decay Mode	Half Life	E_β (MeV)	E_γ (MeV)
^{12}C	98.9%	$^{12}C(^{7}Li,n)^{18}F$	5.96	β^+	110 min	0.63	0.51
^{13}C	1.1%	$^{13}C(^{7}Li,p)^{19}O$	7.41	β^-	27 s	4.60	0.20 1.36
		$^{13}C(^{7}Li,\alpha)^{16}N$	9.92	β^-	7.1 s	4.3	6.13
		$^{13}C(^{7}Li,2n)^{18}F$	1.02	β^+	110 min	0.63	0.51
^{27}Al	100%	$^{27}Al(^{7}Li,p)^{33}P$	16.76	β^-	25 da	0.25	-
		$^{27}Al(^{7}Li,d)^{32}P$	8.89	β^-	14 da	1.71	-
		$^{27}Al(^{7}Li,^{3}He)^{31}Si$	5.74	β^-	2.6 hr	1.49	-
		$^{27}Al(^{7}Li,^{6}Li)^{28}Al$	0.48	β^-	2.2 min	2.86	1.78

Table II

Radioactivities Induced by ^{7}Li Ions on Titanium and Vanadium

Target		Nuclear Reaction		Residual Nucleus			
Isotope	Abundance	Reaction	Q-Value (MeV)	Decay Mode	Half Life	E_β (MeV)	E_γ (MeV)
^{46}Ti	8.0%	$^{46}Ti(^{7}Li,n)^{52}Mn$	13.42	β^+	5.7 da	0.57	1.43
		$^{46}Ti(^{7}Li,n)^{52m}Mn$	13.04	β^+	21 min	2.63	1.43
		$^{46}Ti(^{7}Li,d)^{51}Cr$	9.10	ε	28 da	-	0.32
		$^{46}Ti(^{7}Li,\alpha)^{49}V$	16.31	ε	331 da	-	-
		$^{46}Ti(^{7}Li,2n)^{51}Mn$	2.90	β^+	46 min	2.2	0.51
		$^{46}Ti(^{7}Li,\alpha n)^{48}V$	4.76	β^+	16.0 da	0.70	1.31
^{47}Ti	7.5%	$^{47}Ti(^{7}Li,t)^{51}Cr$	6.48	ε	27.7 da	-	0.32
		$^{47}Ti(^{7}Li,2n)^{52}Mn$	4.54	β^+	5.7 da	0.57	1.43
		$^{47}Ti(^{7}Li,2n)^{52m}Mn$	4.16	β^+	21 min	2.63	1.43
		$^{47}Ti(^{7}Li,2p)^{52}V$	6.84	β^-	3.8 min	2.5	1.43
		$^{47}Ti(^{7}Li,\alpha n)^{49}V$	7.44	ε	331 da	-	-
^{48}Ti	73.7%	$^{48}Ti(^{7}Li,n)^{54}Mn$	13.91	ε	312 da	-	0.835
		$^{48}Ti(^{7}Li,^{3}He)^{52}V$	2.93	β^-	3.8 min	2.5	1.43
		$^{48}Ti(^{7}Li,2p)^{53}V$	4.03	β^-	1.6 min	2.4	1.00
^{49}Ti	5.5%	$^{49}Ti(^{7}Li,p)^{55}Cr$	14.17	β^-	3.6 min	2.59	-
		$^{49}Ti(^{7}Li,^{3}He)^{53}V$	3.60	β^-	1.6 min	2.4	1.00
		$^{49}Ti(^{7}Li,\alpha)^{52}V$	15.36	β^-	3.8 min	2.5	1.43
		$^{49}Ti(^{7}Li,2n)^{54}Mn$	5.76	ε	312 da	-	0.835
		$^{49}Ti(^{7}Li,2p)^{54}V$	1.40	β^-	43 s	3.0	2.21

continued

Table II Continued

Radioactivities Induced by ^{7}Li Ions on Titanium and Vanadium

Target		Nuclear Reaction		Residual Nucleus			
Isotope	Abundance	Reaction	Q-Value (MeV)	Decay Mode	Half Life	E_β (MeV)	E_γ (MeV)
^{50}Ti	5.3%	$^{50}Ti(^{7}Li,n)^{56}Mn$	12.31	β^-	2.6 hr	2.85	0.847
		$^{50}Ti(^{7}Li,p)^{56}Cr$	11.48	β^-	5.9 min	1.5	0.083
		$^{50}Ti(^{7}Li,d)^{55}Cr$	5.45	β^-	3.6 min	2.59	-
		$^{50}Ti(^{7}Li,\alpha)^{53}V$	13.23	β^-	1.6 min	2.4	1.00
		$^{50}Ti(^{7}Li,\alpha n)^{52}V$	4.42	β^-	3.8 min	2.5	1.43
^{51}V	99.8%	$^{51}V(^{7}Li,p)^{57}Mn$	12.90	β^-	1.6 min	2.56	0.122
		$^{51}V(^{7}Li,d)^{56}Mn$	6.48	β^-	2.58 hr	2.85	0.847
		$^{51}V(^{7}Li,^{3}He)^{55}Cr$	2.89	β^-	3.6 min	2.59	-
		$^{51}V(^{7}Li,2p)^{56}Cr$	3.42	β^-	5.9 min	1.5	0.083
		$^{51}V(^{7}Li,^{6}Li)^{52}V$	0.06	β^-	3.8 min	2.5	1.43

Table III

Radioactivities Induced by ^{7}Li Ions on Chromium, Iron and Nickel

Target		Nuclear Reaction		Residual Nucleus			
Isotope	Abundance	Reaction	Q-Value (MeV)	Decay Mode	Half Life	E_β (MeV)	E_γ (MeV)
^{52}Cr	83.8%	$^{52}Cr(^{7}Li,n)^{58}Co$	11.26	ε,β^+	71 da	0.47	0.81
		$^{52}Cr(^{7}Li,^{3}He)^{56}Mn$	1.47	β^-	2.6 hr	2.85	0.847
		$^{52}Cr(^{7}Li,2n)^{57}Co$	2.69	ε	271 da	-	0.122
		$^{52}Cr(^{7}Li,2p)^{57}Mn$	2.40	β^-	1.6 min	2.56	0.122
		$^{52}Cr(^{7}Li,\alpha n)^{54}Mn$	4.55	ε	312 da	-	0.835
^{54}Fe	5.8%	$^{54}Fe(^{7}Li,n)^{60}Cu$	8.94	β^+	23 min	3.77	1.76 1.33
		$^{54}Fe(^{7}Li,^{3}He)^{58}Co$	3.57	ε,β^+	71 da	0.47	0.81
		$^{54}Fe(^{7}Li,\alpha)^{57}Co$	15.58	ε	271 da	-	0.122
		$^{54}Fe(^{7}Li,\alpha n)^{56}Co$	4.20	β^+	77 da	1.46	0.847
		$^{54}Fe(^{7}Li,^{6}Li)^{55}Fe$	2.05	ε	2.7 yr	-	-
^{56}Fe	91.7%	$^{56}Fe(^{7}Li,n)^{62}Cu$	9.04	β^+	9.8 min	2.93	0.51
		$^{56}Fe(^{7}Li,^{3}He)^{60}Co$	1.02	β^-	5.3 yr	0.321	1.17 1.33
		$^{56}Fe(^{7}Li,2n)^{61}Cu$	0.14	β^+	3.4 hr	1.22	0.51
		$^{56}Fe(^{7}Li,2p)^{61}Co$	2.65	β^-	1.65 hr	1.24	0.068
		$^{56}Fe(^{7}Li,\alpha n)^{58}Co$	3.64	ε,β^+	71 da	0.47	0.81

continued

Table III Continued

Radioactivities Induced by ^{7}Li Ions on Chromium, Iron and Nickel

Target		Nuclear Reaction		Residual Nucleus			
Isotope	Abundance	Reaction	Q-Value (MeV)	Decay Mode	Half Life	E_β (MeV)	E_γ (MeV)
^{57}Fe	2.1%	$^{57}Fe(^{7}Li,^{3}He)^{61}Co$	2.73	β^-	1.65 hr	1.24	0.068
		$^{57}Fe(^{7}Li,\alpha)^{60}Co$	13.96	β^-	5.27 yr	0.321	1.17 1.33
		$^{57}Fe(^{7}Li,2n)^{62}Cu$	1.40	β^+	9.8 min	2.93	0.51
		$^{57}Fe(^{7}Li,2p)^{62}Co$	1.68	β^-	14 min	2.88	1.17
		$^{57}Fe(^{7}Li,2p)^{62m}Co$	1.30	β^-	1.5 min	4.1	1.17
^{58}Ni	68.3%	$^{58}Ni(^{7}Li,n)^{64}Ga$	5.54	β^+	2.6 min	6.05	0.51
		$^{58}Ni(^{7}Li,d)^{63}Zn$	3.76	β^+	38 min	2.34	0.51
		$^{58}Ni(^{7}Li,t)^{62}Zn$	0.85	ε,β^+	9.3 hr	0.67	0.51
		$^{58}Ni(^{7}Li,^{3}He)^{62}Cu$	2.56	β^+	9.8 min	2.93	0.51
		$^{58}Ni(^{7}Li,\alpha)^{61}Cu$	14.24	β^+	3.4 hr	1.22	0.51
		$^{58}Ni(^{7}Li,\alpha n)^{60}Cu$	2.56	β^+	23 min	3.77	1.76 1.33
^{60}Ni	26.1%	$^{60}Ni(^{7}Li,n)^{66}Ga$	6.07	β^+	9.5 hr	4.15	0.51
		$^{60}Ni(^{7}Li,d)^{65}Zn$	3.22	ε	245 da	-	1.115
		$^{60}Ni(^{7}Li,^{3}He)^{64}Cu$	0.93	β^- β^+	12.8 hr 12.8 hr	0.575 0.656	- 0.51
		$^{60}Ni(^{7}Li,\alpha n)^{62}Cu$	2.75	β^+	9.8 min	2.93	0.51

Table IV

Radioactivities Induced by ^{7}Li Ions on Copper and Zinc

Target		Nuclear Reaction		Residual Nucleus			
Isotope	Abundance	Reaction	Q-Value (MeV)	Decay Mode	Half Life	E_β (MeV)	E_γ (MeV)
^{63}Cu	69.1%	$^{63}Cu(^{7}Li,n)^{69}Ge$	8.35	ε,β^+	39 hr	1.20	0.51
		$^{63}Cu(^{7}Li,d)^{68}Ga$	3.26	β^+	68 min	1.90	0.51
		$^{63}Cu(^{7}Li,t)^{67}Ga$	1.24	ε	78 hr	-	0.093
		$^{63}Cu(^{7}Li,\alpha n)^{65}Zn$	4.75	ε	245 da	-	1.115
		$^{63}Cu(^{7}Li,^{6}Li)^{64}Cu$	0.66	β^- β^+	12.8 hr 12.8 hr	0.575 0.656	- 0.51
^{65}Cu	30.9%	$^{65}Cu(^{7}Li,n)^{71}Ge$	9.47	ε	11 da	-	-
		$^{65}Cu(^{7}Li,d)^{70}Ga$	3.40	β^-	21 min	1.65	-
		$^{65}Cu(^{7}Li,^{3}He)^{69}Zn$	1.14	β^-	57 min	0.91	-
^{64}Zn	48.9%	$^{64}Zn(^{7}Li,n)^{70}As$	5.16	β^+	50 min	2.1	1.04
		$^{64}Zn(^{7}Li,d)^{69}Ge$	2.87	ε,β^+	39 hr	1.20	0.51
		$^{64}Zn(^{7}Li,t)^{68}Ge$	0.53	ε	287 da	-	-
		$^{64}Zn(^{7}Li,^{3}He)^{68}Ga$	1.05	β^+	68 min	1.90	0.51
		$^{64}Zn(^{7}Li,\alpha)^{67}Ga$	13.35	ε	78 hr	-	0.093
		$^{64}Zn(^{7}Li,\alpha n)^{66}Ga$	2.12	β^+	9.5 hr	4.15	0.51
		$^{64}Zn(^{7}Li,^{6}Li)^{65}Zn$	0.74	ε	245 da	-	1.115

continued

Table IV Continued

Radioactivities Induced by ^{7}Li Ions on Copper and Zinc

Target		Nuclear Reaction		Residual Nucleus			
Isotope	Abundance	Reaction	Q-Value (MeV)	Decay Mode	Half Life	E_β (MeV)	E_γ (MeV)
^{66}Zn	27.8%	$^{66}Zn(^{7}Li,n)^{72}As$	6.17	β^+	26 hr	2.50	0.835
		$^{66}Zn(^{7}Li,d)^{71}Ge$	2.79	ε	11 da	-	-
		$^{66}Zn(^{7}Li,^{3}He)^{70}Ga$	-0.01	β^-	21 min	1.65	-
		$^{66}Zn(^{7}Li,\alpha n)^{68}Ga$	2.60	β^+	68 min	1.90	0.51
^{68}Zn	18.6%	$^{68}Zn(^{7}Li,n)^{74}As$	7.70	ε,β^+	18 da	1.53	0.60
				β^-	18 da	1.35	0.64
		$^{68}Zn(^{7}Li,2p)^{73}Ga$	0.08	β^-	4.9 hr	1.19	0.29
		$^{68}Zn(^{7}Li,\alpha n)^{70}Ga$	3.31	β^-	21 min	1.65	-

energy. On the other hand, lithium-induced reactions are inhibited by a repulsive Coulomb barrier between the incident lithium nucleus and the target nucleus. For a nucleus of atomic number Z_1 and mass number A_1 incident on a target of atomic number Z_2 and mass number A_2, the energy of this barrier is $E_b(MeV) = 1.44Z_1Z_2/R$ where R is expressed in fermis and is given by $R = 1.2(A_1^{1/3} + A_2^{1/3})$. The value of this barrier is listed in Table V for each target element. For elements consisting of several stable isotopes, the most abundant isotope is used. For incident energies below the barrier, the lithium must tunnel quantum-mechanically through the barrier to initiate a nuclear reaction. The probability for tunneling increases rapidly with increasing energy below the barrier. Therefore, for medium-weight targets (Ti to Zn) where E_b is comparable to or larger than 15 MeV, cross sections for lithium-induced reactions below 15 MeV are expected to be small and to increase rapidly as the incident lithium energy increases. For carbon and aluminum targets, the Coulomb barrier is exceeded for incident energies greater than 5.1 and 9.5 MeV, respectively. If the ^7Li energy approaches or exceeds these barrier heights, appreciable radioactivity may be produced by reactions on these targets.

In a survey of the published literature, measured cross sections or thick-target yields in the energy range of interest were found only for the $^{12}C(^7Li,n)^{18}F$ reaction.[5,6] No cross sections or thick-target yields were found for the other reactions listed in Tables I through IV. Thick-target yields or cross sections have been measured for lithium-induced reactions on other low-atomic-number targets (i.e., ^6Li, ^7Li, ^9Be, ^{10}B, ^{14}N, ^{16}O, ^{19}F and ^{23}Na) in the energy range below 15 MeV.[5-7] Invariably, these results indicate that the reaction yields increase rapidly with increasing lithium energy until the incident energy becomes comparable with the Coulomb barrier. This behavior suggests that the reactions in this survey are dominated by Coulomb-barrier effects in the energy range of interest.

To estimate the magnitude of Coulomb-barrier inhibition, the barrier penetrability for ^7Li is evaluated for the different

Table V

Coulomb Barrier Energies for ^{7}Li
on Different Target Nuclei

Target	Z_2	A_2	E_b (MeV)
C	6	12	5.14
Al	13	27	9.52
Ti	22	48	14.3
V	23	51	14.7
Cr	24	52	15.3
Fe	26	56	16.3
Ni	28	58	17.4
Cu	29	63	17.7
Zn	30	64	18.3

targets in this survey. In general, the barrier penetration factor is expressed in terms of tabulated Coulomb functions.[8] However, an analytic expression can be obtained for s-waves in the WKB approximation.[9] In this approximation it is assumed that the wave function of the incoming lithium is slowly varying in the region under the barrier. In this region, the wave function is not sinusoidal, but exponentially decaying. The WKB approximation is good if the lithium energy is close to the barrier potential, E_b, and deteriorates as the lithium energy decreases. We use the analytic WKB expression for the barrier penetration factor to compare reaction yields for different targets with lithium energies near E_b. If the incoming lithium is not described by an s-wave, an additional angular momentum barrier should be included. Neglecting this barrier results in larger penetrations and larger yield estimates.

In the WKB approximation, the s-wave Coulomb-barrier penetration factor[9] is given by $P = \exp(-\gamma)$ where

$$\gamma = 8\pi Z_1 Z_2 e^2/(hv)[\cos^{-1}(T/E_b)^{\frac{1}{2}} - (T/E_b)^{\frac{1}{2}}(1-T/E_b)^{\frac{1}{2}}]. \qquad (1)$$

In this expression, $T = \frac{1}{2}\mu v^2$ is the incident ^{7}Li energy, and $\mu = A_1 A_2/(A_1+A_2)$ is the reduced mass. This penetration factor is presented in Figs. 1 and 2 as a function of the ^{7}Li energy for the targets in this survey. The values of Z_2 and A_2 listed in Table V are used for these calculations. The penetration factors are expressed in yield units by normalizing the carbon-target penetration factor to measured thick-target yields[6] for the $^{12}C(^7Li,n)^{18}F$ reaction on a carbon target in the range from 2.5 to 3.5 MeV. For the targets in Fig. 1, the penetration factors extend up to the Coulomb barrier. As the atomic number of the target is increased, these curves shift to higher ^{7}Li energy. For the targets in Fig. 2, the Coulomb barriers are larger than 15 MeV (see Table V). Again, the penetration factors shift to higher ^{7}Li energy as the atomic number of the target is increased.

The curves in Figs. 1 and 2 are intended to show the trend in reaction yield due to the Coulomb barrier. Thick-target

yields of up to 10^{-5} reactions/^{7}Li can be expected for carbon and aluminum. Somewhat lower yields are estimated for the higher atomic number targets. Actual yields may be larger or smaller than these estimates due to different nuclear reaction mechanisms and due to different internal structures of the target and final nuclei in the reactions.[10,11] For example, a reaction such as (^{7}Li,n) requires that all of the charged particles in the ^{7}Li be transferred to the target to form the final nucleus. Such a reaction may be expected to proceed through the formation of a compound nucleus. In this case, the reaction is inhibited by the Coulomb barrier as previously described. On the other hand, a reaction such as (^{7}Li,^{6}Li) may proceed by simply transferring a neutron; the charged particles in the ^{7}Li need not penetrate the Coulomb barrier but only get sufficiently close to the target for neutron transfer to occur. Coulomb-barrier inhibition is less in this case. In the present survey, the largest Q-values tend to occur for (^{7}Li,n) and (^{7}Li,p) reactions which have the largest barrier inhibitions. The less inhibited (^{7}Li,^{6}Li) reactions tend to have small positive Q-values, and the (^{7}Li,^{6}He) reactions have negative Q-values. These kinematic trends suggest that effects due to different nuclear reaction mechanisms are not likely to overwhelm the trends due to Coulomb-barrier inhibition.

The (^{7}Li,α) and (^{7}Li,t) reactions are favored by the internal structure of ^{7}Li. The ^{7}Li nucleus has a significant (α+t) cluster structure so that these reactions may proceed by the transfer of either an α-particle or a triton from the ^{7}Li to the target.[10,11] These cluster-transfer reactions resemble stripping reactions which proceed selectively to ground and excited states of the final nucleus which have the appropriate cluster structure. To evaluate the probability of such reactions requires detailed knowledge of the nuclear structure of the target and of the final nucleus and is beyond the scope of this survey.

In conclusion, nuclear reactions, which are induced by up to 15-MeV ^{7}Li ions and which produce radioactivity, are surveyed for several commonly used target materials: carbon, aluminum, steel, brass, and a titanium alloy. Positive Q-value reactions

are identified along with the decay properties of the radioactive nuclei. Yields for these reactions are dominated by penetration of the Coulomb barrier in the entrance channel. Barrier-penetration calculations indicate the reaction yields decrease as the atomic number is increased and increase rapidly with ^{7}Li energy up to the Coulomb barrier.

Acknowledgements

The encourgement of John Maenchen of Sandia National Laboratories to carry out this survey is appreciated. This work was supported by the Department of Energy through Sandia National Laboratories.

REFERENCES

1. K.A. Keller, J. Lange and H. Münsel, in Landbolt-Bornstein Numerical Data and Functional Relationships in Science and Technology Vol. 5, Part a, Q-Values, edited by H. Schopper (Springer-Verlag, New York, 1973).
2. Chart of the Nuclides, Knolls Atomic Power Laboratory, 11th Edition, April, 1972.
3. C.M. Lederer, J.M. Hollander and I. Perlman, Table of Isotopes, 6th Edition (John Wiley, New York, 1967).
4. J.B. Marion and F.C. Young, Nuclear Reaction Analysis (North-Holland, Amsterdam, 1968), p. 157.
5. E. Norbeck, Jr. and C.S. Littlejohn, Phys. Rev. 108, 754 (1957).
6. E. Norbeck, Phys. Rev. 121, 824 (1961).
7. R.R. Carlson and H.W. Wyborny, Phys. Rev. 178, 1529 (1969); D.J. Johnson and M.A. Waggoner, Phys. Rev. C 2, 41 (1970); H.W. Wyborny and R.R. Carlson, Phys. Rev. C 3, 2185 (1971).
8. J.M. Blatt and V.F. Weisskopf, Theoretical Nuclear Physics (John Wiley, New York, 1952), Chapt. 8.
9. R.D. Evans, The Atomic Nucleus (McGraw Hill, New York, 1955) pp. 874-6.
10. R.R. Carlson, "Lithium Induced Reactions," in Nuclear Research with Low Energy Accelerators, J.B. Marion and D.M. Van Patter, Eds. (Academic Press, New York, 1967), pp. 475-496.
11. A.A. Ogloblin, "The Study of Lithium-Induced Reactions at the Kurchatov Atomic Energy Institute," in Nuclear Reactions Induced by Heavy Ions, R. Bock and W.R. Hering, Eds. (North Holland, Amsterdam, 1970), pp. 231-262.

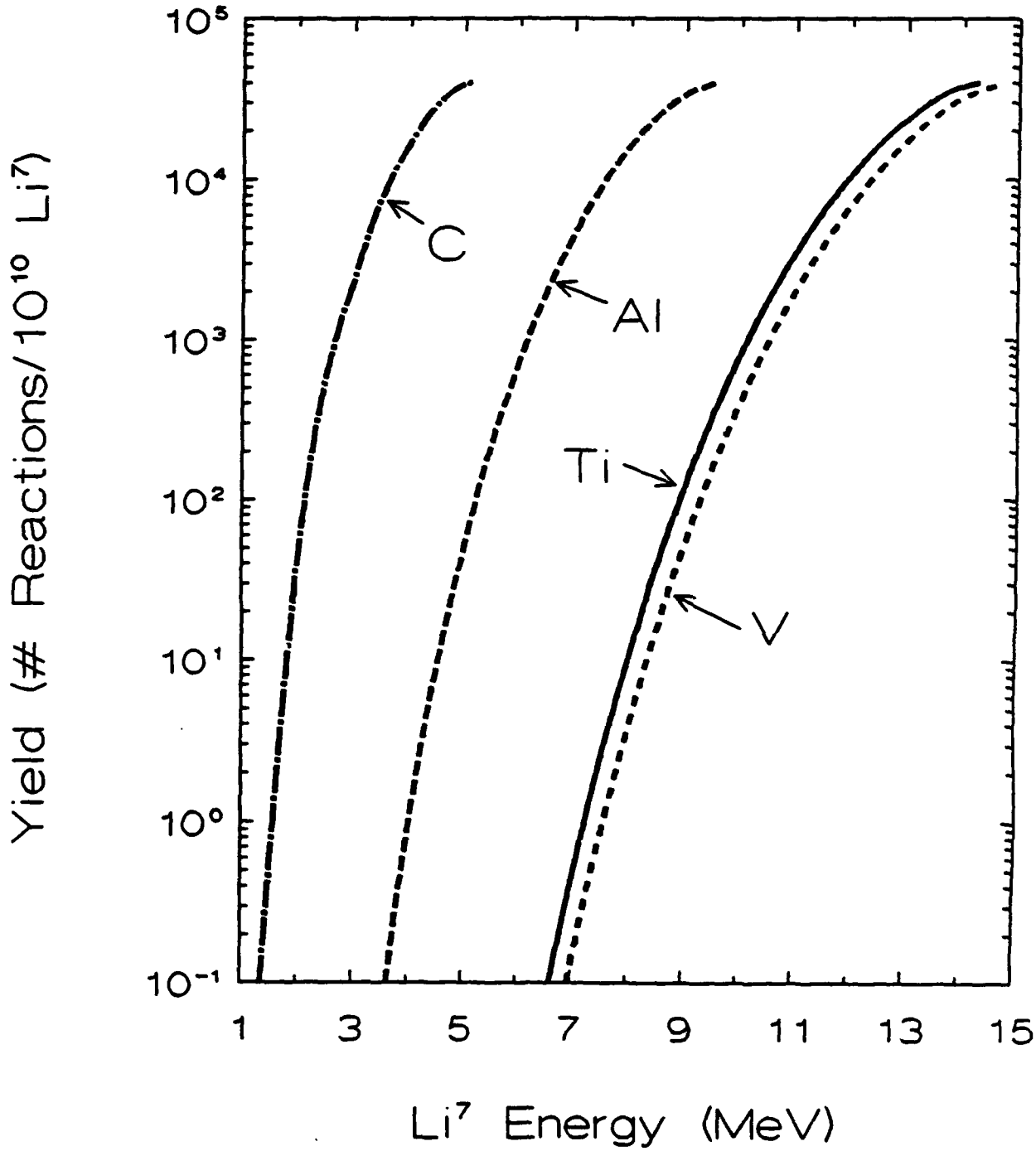

Fig. 1. Coulomb barrier penetration factors for ^{7}Li nuclei incident on carbon, aluminum, titanium and vanadium targets. The penetration factor is expressed in yield by normalizing to measured thick-target yields for the $^{12}C(^{7}Li,n)^{18}F$ reaction.

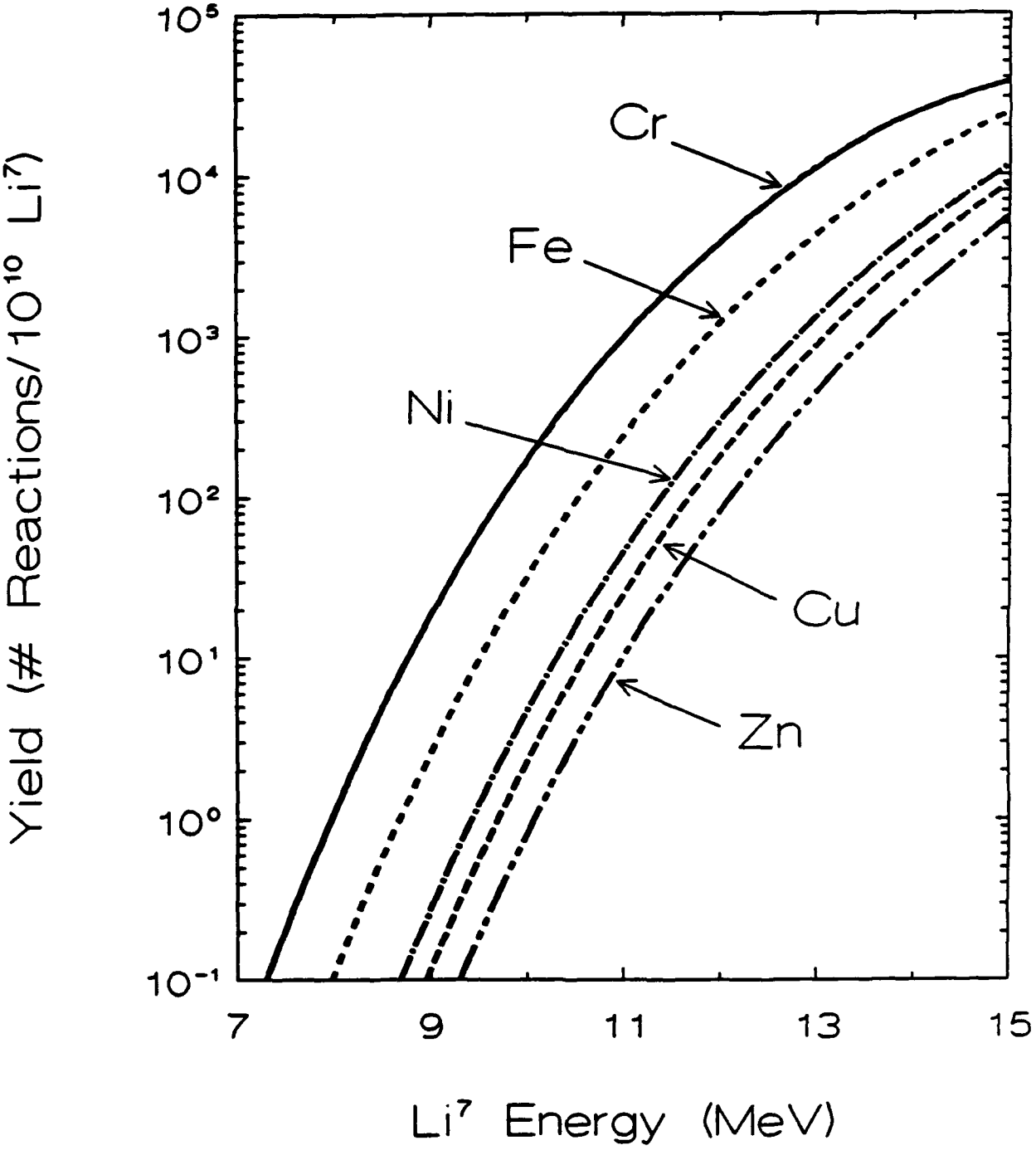

Fig. 2. Coulomb barrier penetration factors for ^{7}Li nuclei incident on chromium, iron, nickel, copper and zinc targets. The penetration factor is expressed in yield by normalizing to measured thick-target yields for the $^{12}C(^{7}Li,n)^{18}F$ reaction.